

Tri-layered composite plug for the repair of osteochondral defects: in vivo study in sheep

Journal of Tissue Engineering
Volume 8: 1–10
© The Author(s) 2017
Reprints and permissions:
sagepub.co.uk/journalsPermissions.nav
DOI: 10.1177/2041731417697500
journals.sagepub.com/home/tej



Altug Yucekul¹, Deniz Ozdil^{2,3}, Nuri Hunkar Kutlu²,
Esra Erdemli⁴, Halil Murat Aydin⁵ and Mahmut Nedim Doral¹

Abstract

Cartilage defects are a source of pain, immobility, and reduced quality of life for patients who have acquired these defects through injury, wear, or disease. The avascular nature of cartilage tissue adds to the complexity of cartilage tissue repair or regeneration efforts. The known limitations of using autografts, allografts, or xenografts further add to this complexity. Autologous chondrocyte implantation or matrix-assisted chondrocyte implantation techniques attempt to introduce cultured cartilage cells to defect areas in the patient, but clinical success with these are impeded by the avascularity of cartilage tissue. Biodegradable, synthetic scaffolds capable of supporting local cells and overcoming the issue of poor vascularization would bypass the issues of current cartilage treatment options. In this study, we propose a biodegradable, tri-layered (poly(glycolic acid) mesh/poly(L-lactic acid)-colorant tidemark layer/collagen Type I and ceramic microparticle-coated poly(L-lactic acid)-poly(ϵ -caprolactone) monolith) osteochondral plug indicated for the repair of cartilage defects. The porous plug allows the continual transport of bone marrow constituents from the subchondral layer to the cartilage defect site for a more effective repair of the area. Assessment of the in vivo performance of the implant was conducted in an ovine model ($n = 13$). In addition to a control group (no implant), one group received the implant alone (Group A), while another group was supplemented with hyaluronic acid (0.8 mL at 10 mg/mL solution; Group B). Analyses performed on specimens from the in vivo study revealed that the implant achieves cartilage formation within 6 months. No adverse tissue reactions or other complications were reported. Our findings indicate that the porous biocompatible implant seems to be a promising treatment option for the cartilage repair.

Keywords

Osteochondral repair, cartilage repair, polyglycolic acid, poly-L-lactic acid, beta-tricalcium phosphate, hyaluronic acid

Date received: 13 December 2016; accepted: 12 February 2017

Introduction

Articular cartilage that has been damaged due to injury, disease, or wear has, by nature, a very limited capacity for self-healing as cartilage is a predominantly avascular tissue.¹ Aging, obesity, and physical activity exacerbate articular cartilage defects in the knee. While manifesting symptomatically as extreme pain in the knee, these defects eventually lead to the immobility of the patient and ultimately a reduction in their quality of life. Untreated lesions most commonly eventuate in the need for total knee replacement and there are approximately 600,000 total knee replacement procedures performed in the U.S every year.² This figure is indicative of the significance of

¹Department of Orthopedics and Traumatology, Faculty of Medicine, Hacettepe University, Ankara, Turkey

²BMT Calsis Health Technologies Co., Ankara, Turkey

³Bioengineering Division, Institute of Science and Engineering, Hacettepe University, Ankara, Turkey

⁴Department of Histology and Embryology, School of Medicine, Ankara University, Ankara, Turkey

⁵Environmental Engineering Department & Bioengineering Division and Centre for Bioengineering, Hacettepe University, Ankara, Turkey

Corresponding author:

Halil Murat Aydin, Environmental Engineering Department & Bioengineering Division and Centre for Bioengineering, Hacettepe University, 06800, Ankara, Turkey.
Email: hmaydin@hacettepe.edu.tr



Creative Commons Non Commercial CC BY-NC: This article is distributed under the terms of the Creative Commons

Attribution-NonCommercial 3.0 License (<http://www.creativecommons.org/licenses/by-nc/3.0/>) which permits non-commercial use, reproduction and distribution of the work without further permission provided the original work is attributed as specified on the SAGE and Open Access page (<https://us.sagepub.com/en-us/nam/open-access-at-sage>).

developing viable and effective cartilage defect treatments. Current treatment options include microfracture surgery, autografting, and allografting; however, these options have drawbacks such as prolonged healing times, donor site morbidity, and availability and compatibility issues, respectively. The composition and structure of cartilage tissue further adds to this complexity.

There are three types of cartilage found in the body, varying in terms of biochemical constituents, structure, and location. Elastic cartilage is found in the outer ear and larynx and approximately 20% of its dry weight is elastin. Fibrous cartilage has lower amounts of glycosaminoglycan (GAG) but more organized fibers. Hyaline cartilage is particular to the knee joint with a thickness of 0.5–0.7 mm and offers a low friction and load distribution surface between bones. Generally, cartilage is composed of 95% extra cellular matrix (ECM) and 3%–5% chondrocytes. About 60%–80% of the ECM is water. Hyaline cartilage, containing only one cell type and no vascular or lymphatic networks, is one of the simplest tissues within the body. This tissue is composed of scattered chondrocytes in an ECM, a fibrous network collagen Type II, proteoglycans, and water. The GAG/proteoglycan aggregates of hyaline cartilage, which make up 15%–30% of its dry weight, form hydrophilic gels capable of retaining large amounts of water, thereby giving this tissue a high compressive strength.³

If hyaline cartilage is torn or damaged, any joint movement will be severely limited and associated with pain. Damaged cartilage tissue generally attempts repair by producing Type I collagen, leading to the formation of fibrotic tissue. Due to the weak mechanical compressive strength of this fibrous structure, it wears away also with time, and the joint continues to experience damage. Initially becoming swollen and endemic, the joint will eventually see the formation of cysts and deeper lesions. The final stage usually involves the lesions deepening enough to reach subchondral bone tissue. It is believed that these lesions progressively develop into osteoarthritic forms. Osteoarthritis is the leading cause of immobility and injury in the middle-aged and elderly population. It also brings with it social, psychological, and economic expenses. Each year over 39 million people visit the doctor due to osteoarthritis-related conditions, with 500,000 of these requiring hospitalization. In the United States, it is expected that by 2020 over 60 million people will be affected and 11.6 million people will experience limitations to their activities as a consequence of arthritis.⁴ Current therapeutic approaches toward cartilage repair depend on several factors such as defect size and patient status and are summarized in Table 1.

In this study, a biocompatible, biodegradable, porous three-dimensional (3D) osteochondral plug capable of repairing articular cartilage defects was tested in ovine cartilage defect models. Due to its functional design cell seeding onto the structure prior to surgery is no longer required

as the vertical microchannels running through the plug are designed to provide the continual supply of bone marrow constituents to the articular cartilage layer. The plug is tri-layered with the top layer being composed of a nonwoven poly(glycolic acid) (PGA) felt, the middle layer is poly(L-lactic acid) (PLLA) mixed with a colorant, and a bottom layer is composed of a porous poly(L-lactic acid)/poly(ϵ -caprolactone) (PLLA/PCL) structure coated with collagen Type I and beta-tricalcium phosphate (β -TCP) microparticles. The top and bottom layers are designed to mimic cartilage and bone tissue, respectively, and provide an ideal environment for the infiltration, attachment, and proliferation of the respective cell types. The middle layer not only provides a visual aid during implantation but also acts as a selective barrier for the two different cell types to be involved in the tissue regeneration process. The microchannels within the plug allow the continuous supply of bone marrow constituents to the cartilage layer throughout the healing period. The tri-layered osteochondral plug is completely resorbable and will eventually be replaced by new healthy tissue. This study provides results of the in vivo ovine performance of the tri-layered implants.

Materials and methods

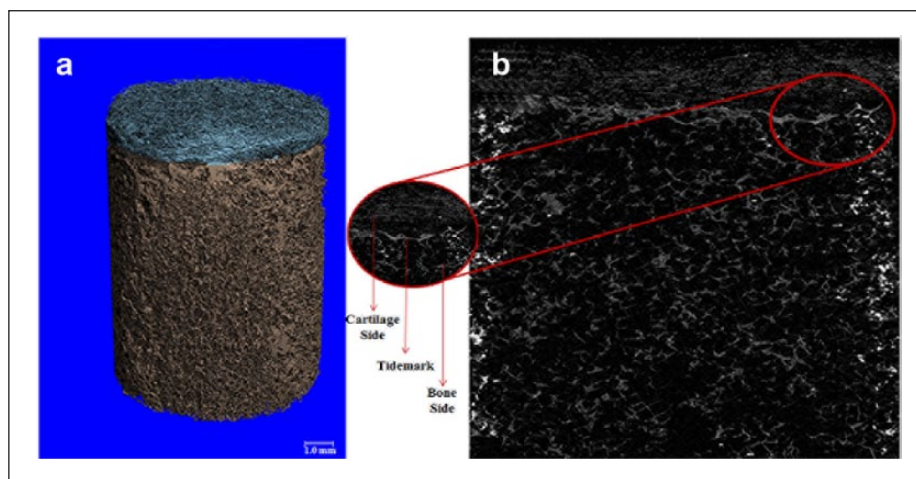
Scaffold preparation

A detailed description of the scaffold preparation protocol is given in our previous work.¹⁵ The top layer of the three-layered scaffold is composed of a nonwoven poly(glycolic acid) (PGA) felt (Suprachon; BMT Calsis, Turkey). The bottom layer is a porous structure composed of a blend of (PLLA; $M_w=220$ kDa) and PCL ($M_w=65$ kDa). Briefly, dried flakes of PLLA and PCL were dissolved in chloroform (12% w/v) and then precipitated in methanol. A porogen (NaCl, sieved, particle size: 250–300 μ m) was added to the mixture. All constituents were mixed inside a mold. Solvent and porogen removal was achieved via vacuum and leaching with deionized water (DI water), respectively. The monoliths were then subjected to supercritical carbon dioxide (scCO₂) treatment at 150 atm and 38°C for 10 min (a detailed description of the process is given in a previous study).¹⁶ The monoliths were cut into $\varnothing 8 \times 8$ -mm cylinders. The cylinders were then coated with Type I collagen (2 mg/mL; Serva, Germany) and β -TCP (average particle size: 25–45 μ m). The densities per monolith were 100 mL (in 250 mL, 0.1 M acetic acid) and 8 mg for the collagen and β -TCP, respectively. The middle tier of the monolith is a tidemark zone fabricated from a pigmented (Solvent Blue, 3% w/v; Sigma, United Kingdom) PLLA (5% w/v) and is used to adhere the PGA layer to the PLLA construct. It also provides a visual aid for implantation.¹⁵ Vertical channels running throughout the structure were formed manually using stainless steel pins (300 μ m diameter). Figure 1 displays a micro-computed tomography

Table 1. The current approaches used in the treatment of cartilage and osteochondral defects.

Method	Notes
Lavage/arthroscopic cleaning with NaCl/Ringer's solution	Alleviate pain. The effects are only temporary. No healing achieved in later stages.
Debridement ⁵	Symptomatic relief. Not stimulate chondrogenesis or repair.
Abrasion arthroplasty and drilling ^{6,7}	Achieve formation of fibrous, hyaline-like cartilage. Drilling is more effective. No full healing.
Osteotomy ⁸	Involves the manual realignment of cartilage surface by interrupting the bone at a distance from the cartilage lesions.
Total knee replacement procedures ⁹	Performed in more aged patients as the life time of the prosthetics is limited by its loosening with time, and a significant amount of bone loss and pain is associated with prosthetic joints.
Microfracture ¹⁰	Involves the stimulation of repair using microfractures through which the bone marrow is drawn from the subchondral bone. The fibrous and mechanically weak tissue which forms in this way provides only a temporary solution.
Autologous chondrocyte transplantation (ACT) ¹¹	Approximately 10–12 million cells can be implanted into a 10-cm ² defect area. Rehabilitation in the postoperative period is of importance. Complications include the postoperative problems that may form with arthrotomy, the inability to successfully suture periosteal tissue to defect sites, and the delayed hypertrophic response of the body.
Osteochondral transplantation or mosaicplasty ^{12,13}	Involves transplanting healthy tissues containing the required cells from a donor site to areas where they are needed. Disadvantages include donor site morbidity, abrasion against surfaces opposite to the graft, and damage to chondrocytes within donor and recipient regions.
Scaffolds/matrices (polymeric or composite), MACI ¹⁴	Cells proliferated on the matrix and then this structure is delivered to the defect site. Disadvantages include the loss of phenotypic features of chondrocytes and the inability to homogeneously distribute these cells.
Stem cells delivered within 3D matrices	The key criteria include biocompatibility, porosity, biodegradability, and the ability to prevent phenotypic losses in cells and enabling their uniform distribution. Poor cell distribution and mechanical strength are the two main limiting factors for the uptake of such matrices.

MACI: matrix-assisted chondrocyte implantation; 3D: three-dimensional.

**Figure 1.** (a) Micro-CT images of the osteochondral plugs and (b) a cross-sectional view revealing the layered structure.

(CT) image of the plugs prepared by the process described in the previous study.¹⁵

In vivo studies

The ethical approval for the animal study was received from Çukurova University Medical Sciences Experimental Research and Application Center (TIBDAM-1.08.10.2012).

The *in vivo* study was performed at Çukurova University by Dr Altug Yucekul (Hacettepe University Faculty of Medicine), under the supervision of Veterinarian Associate Prof. Dr Kenan Dagoglu (Çukurova University Medical Sciences Experimental Research and Application Center). The osteochondral plugs were implanted into the lateral condyles of the hind right knees of 13 sheep (Merinos breed) via lateral parapatellar arthrotomy with medial

patellar luxation (see Supplementary Information SI-1). In the control group ($n=3$), the defects created ($\varnothing 8$ mm, 10 mm depth) were left open. The remaining animals were divided into two groups, namely, Group A ($n=5$) and Group B ($n=5$). Group B animals received hyaluronic acid gel injected to the osteochondral plugs. Arthroscopic analysis of the joints was performed at 3 months in one control and three Group A animals. The samples obtained (inclusive of the entire knee area) from the animals sacrificed at 3 months (Group A, $n=3$) were analyzed with CT, followed by a histological analysis with methylene blue staining of cartilage areas on the condyle where tissue repair was seen. Three groups of specimens were fixed with 10% buffered formalin (pH: 7.4) in room temperature at 48 h and then were washed in slowly running tap water for 1 h. A 1:1 (v/v) solution of 8% HCl and 8% formic acid was used for decalcification. When fully decalcified, specimens were routinely prepared for light microscopy and embedded in paraffin. Then, 5- μ m-thick serial sections were taken, and nuclei were stained with 4',6-diamidino-2-phenylindole (DAPI) for aggrecan and collagen, hematoxylin/eosin (HE) staining performed for routine examination, and Mallory trichrome for connective tissue. Immunohistochemical staining was also done for collagen II and aggrecan. Photomicrographs of each sample were generated by a light microscope with fluorescence attachment (Axio Scope.A1; Carl Zeiss, Jena, Germany) attached with a computerized digital camera (AxioCam MRc5).

At 6 months post-implantation, samples of the entire knee region obtained from all of the animals sacrificed were analyzed with magnetic resonance imaging (MRI), followed by arthroscopic imaging. Good health was observed in all animals throughout the duration of the experiment; however, the animals of the experimental groups appeared to move more comfortably compared to those of the control group for which limping was reported in the first 3 weeks post-surgery.

Results

In vivo outcomes (analyses at the third month)

Arthroscopy was performed on Group A specimens by entering through the medial and lateral portals 1 cm proximal to the tibial crest. Arthroscopic analysis of the full knee samples from animals sacrificed after 3 months post-implantation of the composite repair matrix revealed a minimum coverage of 50% and a maximum coverage of 80% (according to the defect size) by newly formed tissue. Figure 2 shows that the 8 mm defects initially created were found to be reduced down to 3–4 mm (as seen according to the ruler in Figure 2; about 75% reduction in surface area) in the form of a narrowing crater. No degeneration in other compartments was observed in arthroscopic analyses at 3 months.

According to the CT results, the femoral joint surfaces appeared normal. In the lateral sections of the joints,



Figure 2. Arthroscopic image taken from Merinos sheep with composite scaffold implantation (Group A) sacrificed at 3 months.

defects similar to those observed with arthroscopy were found. Compared to the control groups, 65%–80% reduction of defect sites were observed in animals that received the implants. Arthroscopic findings indicate a significant degree of healing of the defect. A video of the CT analysis has been given in the Supplementary Information (SI-2).

Analyses at 6 months

Macroscopic analysis. General analyses performed during the sacrifice of the animals found that there had been no healing or positive development at the defect sites in the control group animals (Figure 3(a)). Comparatively, the support matrix had achieved tissue regeneration and complete closure of the defect in all of the animals which received the implant. In the control group, the tissue surrounding the defect sites was found to be degenerated due to apoptosis and necrosis, and these effects appeared to continue following sacrifice.

In animals that received the prepared scaffolds, new cartilage tissue with excellent surface and morphology formed within the defect sites. Macroscopic examination of plugs with (Figure 3(c)) and without (Figure 3(b)) hyaluronic supplementation revealed that both implants were capable of maintaining healthy tissue regeneration through the 6-month period. Condylectomy was performed to compare the degree of repair in the bone sections of the osteochondral defects in experimental and control groups, revealing that partial healing was only present in samples that received the implant. Figure 3(d) is a representative image from Group A showing the uniform formation of bone tissue within the bone side of the defect volume. The complete regeneration and repair of these defects was expected at 12 months post-operatively;

however, a follow-up study was not within the means and scope of this study.

Arthroscopic analysis. Arthrotomy was performed by opening the joint. Arthroscopy was performed on samples collected at 6 months to analyze the condition of the defect sites. A clear difference between the control group animals and animals that received the osteochondral implant was observed. The defects created remained open in all control group animals, whereas these defects were completely filled and covered by new cartilage tissue in the experimental animals (Figure 4; see Supplementary Information of arthroscopic videos for Group A, 6 months arthroscopy (SI-3); Group B, 6 months arthroscopy (SI-4); and Group C, 6 months arthroscopy (SI-5).

The defect site and surrounding regions, as well as the trochlea and medial condyles, were analyzed for signs of

degeneration. Possible tissue degeneration in other areas was expected due to the disruption of joint biomechanics in the presence of the defect. Degeneration in the aforementioned areas was seen in samples from the control group (Figure 4(a)); especially in the trochlear region, a similar condition was found in only one of the experimental animal samples. Fibrotic tissue ingrowth was found in defects of control group samples from surrounding soft tissue structures. In one experimental group sample, the defect region was found to be collapsed. When correlated with the MRI images, repair was found to be in the form of a funnel toward the bone marrow. Also, in one animal that received the implant, a thin fracture extending from the condyle toward the periphery was formed while attempting to create the defects. Poor tissue repair and regeneration was found in this particular sample compared to the other implant groups.

MRI. MRI analysis (1.5 Tesla; Siemens Maestro Class, Siemens, Malvern, USA) of all samples taken 15–20 cm above the joint region in all animals confirmed the excellent induction of cartilage formation in the experimental groups. Imaging in the sagittal plane revealed that even at 6 months, the control group defects remained at 7–8 mm, and Figure 5(a) shows that no closure of the defect has been achievable in this group. Where the osteochondral implants are present, new cartilage tissue is found to be level with native cartilage and displays a relatively high density. Group A specimens (Figure 5(b)) show a repair of tissue along the contour line of cartilage.

Histological analyses. In qualitative histological examination of the three groups, the control group had the worst appearance, having failed to fill the defect properly (Figure 6). The defect region had a big cavitation in the center which was surrounded with fibrous connective tissue and increased number of vessels. In some regions, the newly formed cartilage areas were present between the old bone fragments. In the examination of Group A, a central scaffold was seen surrounded with the fibrous connective tissue, with increased vessels and newly forming cartilage

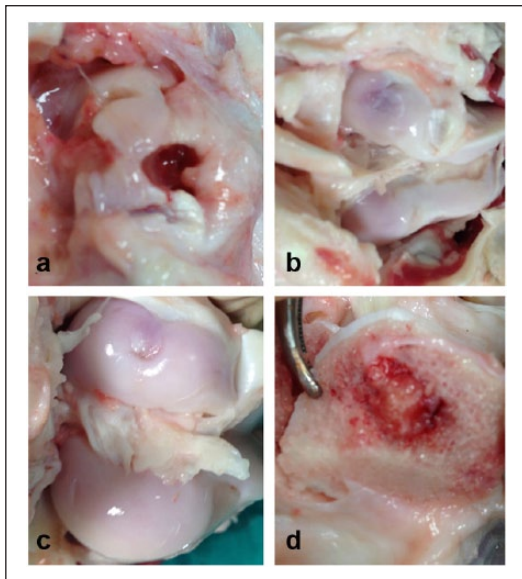


Figure 3. A macroscopic analysis image of the defect sites at 6 months in (a) the control, (b) Group A, and (c) Group B animals, respectively, and (d) the bone side.

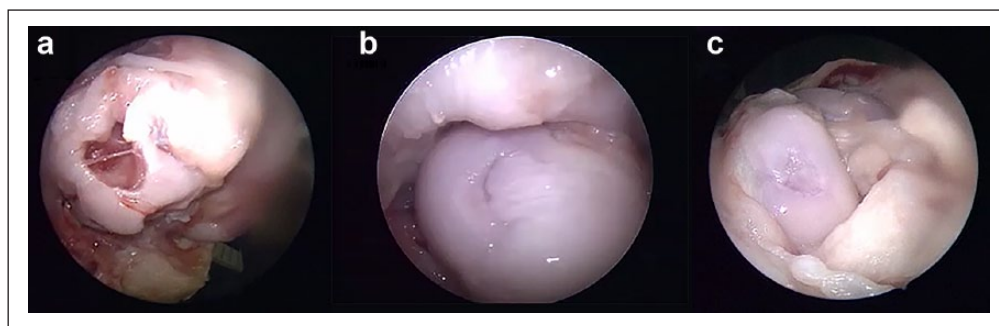


Figure 4. (a) Representative arthroscopic images of knee of the control group, (b) defects with osteochondral plugs, and (c) defects with the osteochondral plug + hyaluronic acid taken at 6 months.

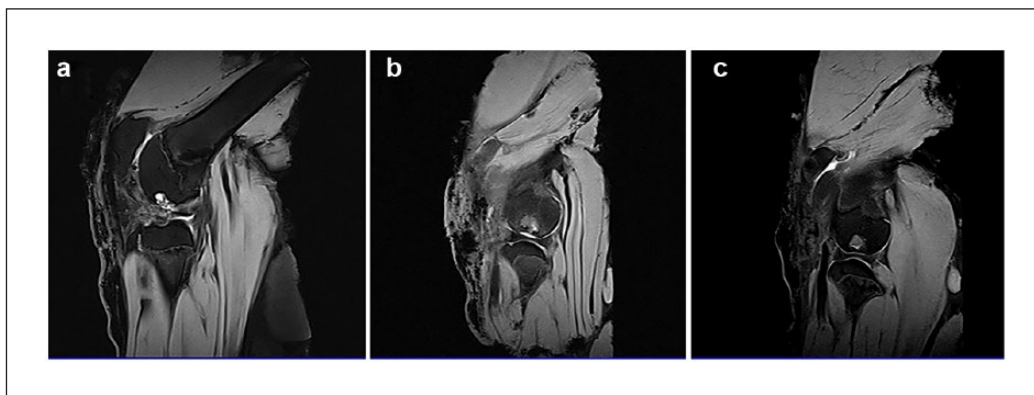


Figure 5. Representative MRI images of (a) the control group, (b) Group A, and (c) Group B.

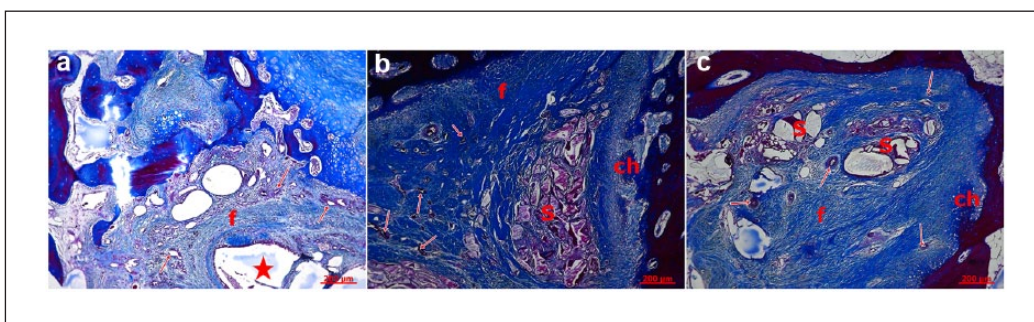


Figure 6. In Mallory trichrome staining: (a) control group, (b) Group A, and (c) Group B. f: fibrous connective tissue; ch: cartilage; S: scaffold; *: cavitation; arrows: vessels.

extensions which appeared to sit on a base of trabecular bone. In Group B, a central scaffold which was surrounded with the thick fibrous tissue was observed with thick collagen bundles. There was an increase in the number of vessels and peripheral cartilage formation under the bone trabeculae indicating the healing process. The repair tissue was formed after initial granulation response, cartilage formation, and remodeling of the subchondral zone. This process was more regular and better in Groups A and B. Defect areas were filled with dense fibrous tissue and round chondrocytes organized in columns in some regions. The major proteoglycan in the articular cartilage is aggrecan. This molecule is important in the proper functioning of the articular cartilage, and it provides a hydrated gel structure. Type II collagen is present in the cartilage and provides resistance to intermittent pressure. Figure 7 and Table 2 give Mallory trichrome staining and semi-quantitative evaluation of the cartilage repair according to a reported evaluation scale for the histological grading of the cartilage repair.¹⁷

The immunohistochemistry results showed that collagen Type II and aggrecan proteins were expressed in the repairing regions; the expressions of which were observed in the cytoplasm of the cells (Figures 7 and 8). These histologic findings revealed increased filling of the defect and

amount of fibrocartilage tissue in Groups A and B when compared to the control group.

Discussion

Osteochondral defects present a further challenge for tissue engineers as both osteogenesis and chondrogenesis must be achieved simultaneously in this case. The tissue regenerative support structure that is to repair such defects must be able to address the requirements of these two structurally, functionally, and constitutionally different tissues. An osteochondral scaffold, therefore, needs distinct architectural features capable of inducing the migration, attachment, and proliferation of different cell lines. The degradation profile of the scaffold must also match the rate of tissue formation in the cartilage and bone layers of the defect separately. Previously, single-phase synthetic osteochondral plugs fabricated from various materials were tested with varying results. Homogeneous scaffolds are, however, insufficient for simultaneously achieving repair in different zones of tissue. Therefore, there has been a gradual movement toward biphasic or functionally graded osteochondral plugs. Figures 3(d) and 5(c) and (d) show the residue of the polymeric scaffold in the bone side, while there was no indication of PGA mesh scaffold

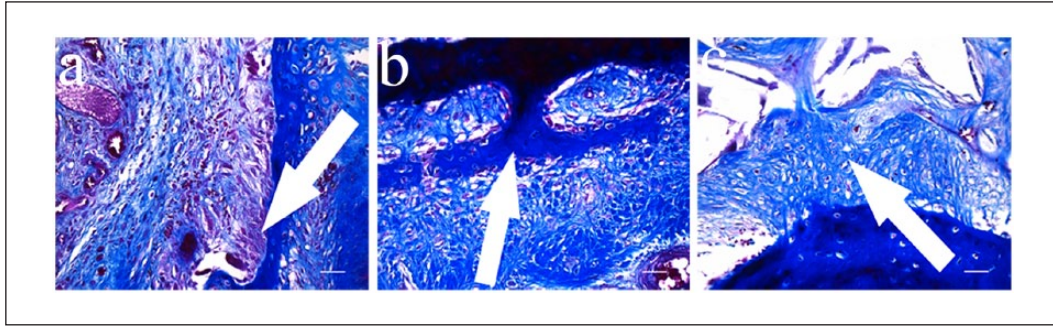


Figure 7. In Mallory trichrome staining: (a) control group, showing only activating cells (\uparrow) going toward fibrous connective tissue; (b) Group A, cartilage tissue which invades fibrocartilage tissue (\uparrow); and (c) Group B, fibrocartilage tissue cells are seen (\uparrow).

Table 2. Semi-quantitative scoring of the cartilage repair.

Parameter	Control	Group A	Group B
I	50% (2)	75% (1)	100% (0)
II	Not close (2)	Almost (1)	Yes (1)
III	Significantly reduced staining (2)	Reduced staining (2)	Normal (1)
IV	Some fibrocartilage but mostly nonchondrocytic cells (3)	Mostly fibrocartilage (2)	Mostly hyaline and fibrocartilage (1)

Scale parameters (I) percent filling of the defect, (II) reconstitution of the osteochondral junction, (III) matrix staining, and (IV) cell morphology with score range starting from 0 (best).

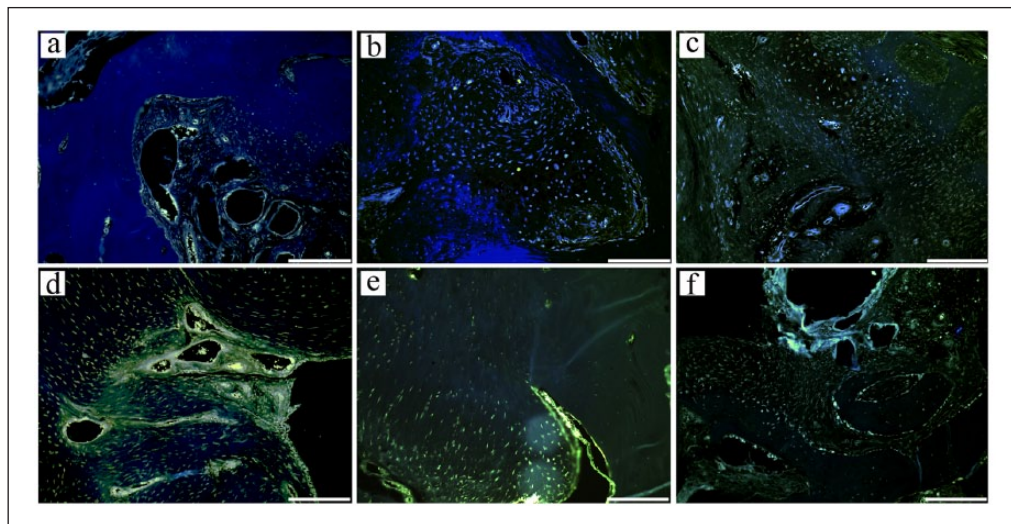


Figure 8. (a–c) Expression of collagen Type II. Tissues were stained using the NorthernLights™ 557-conjugated anti-goat IgG secondary antibody (yellow, Catalog #ab34712) and counterstained with DAPI (blue). Scale bar: 100 μ m; (d–f) Aggrecan immunostaining. Cells were stained using the NorthernLights 557-conjugated anti-goat IgG secondary antibody (yellow, Catalog #ab3773) and counterstained with DAPI (blue). Scale bar: 100 μ m.

observed in the analyses. Considering the scaffold's high porosity (over 90%), it can be concluded that the polymer volume remained in the defect area in the bone side after 6 months does not impose any problem for cartilage regeneration.

Biomimetic biphasic scaffolds, such as the one in this study, are typically composed of a cartilage segment and a

subchondral moiety. While low-strength hydrogels are typically used for the segments interacting with cartilage, mechanically stronger materials such as calcium phosphates and bioceramics are required for the bone-related segments.^{18,19} Previously explored natural materials for this purpose include collagen,²⁰ chitosan,²¹ hyaluronan,²² and alginate.²³ A vast number of materials including poly(lactic

acid) (PLA),²⁴ poly(lactic-glycolic acid) (PLGA),^{23,25} poly(ϵ -caprolactone) (PCL),²⁶ poly(2-hydroxyethyl methacrylate) (PHEMA),²⁷ β -TCP,²⁸ and hydroxyapatite (HA)²⁹ have been used in the repair of cartilage and osteochondral defects. Furthermore, issues such as the poor cell attachment property of some synthetic polymers have been overcome by surface modifications with materials such as chondroitin sulfate³⁰ and chitosan.³¹

For the plug in this study, a polymeric solution mixed with a colorant was used to create a solidified binding segment between the two main layers. The primary aim of this layer is to allow the cells and tissue constituents of the cartilage and bone layers to remain separated. In addition to this, it provides a visual aid during the implantation of the plug. The top collagenous layer is designed to promote mesenchymal stem cell condensation at this site, allowing chondrocyte precursors to form, which in turn will secrete the necessary factors for cartilage ECM formation and cartilage tissue growth. Several studies have shown that not only is it important to induce the involvement of cells in this layer, but supporting the viability and activity of these cells is also critical.^{25,32,33} The hyaline-like cartilage formation at defect site observed in this *in vivo* study can be attributed to the vertical channels in the intermediate binding layer of the scaffold which allowed the transport and lodgment of cells into the topmost layer where they could differentiate into chondrocytes. These channels were also intended to enable and support vascularization throughout the depth of the defect, as well as allowing the mass transfer of nutrients and gases. The ultimate intended function for these channels was to deliver blood from the bone marrow to the upper layers of the defect, imitating Haversian canals in the bone and achieving the same effects as in the microfracture approach. As such, there was active support supplied to the cartilage layer throughout the healing period. This concept is also supported by the study of Chen et al.³⁴ in which a radially oriented collagen scaffold was shown to support *in vivo* cartilage repair, attributed to the induction of stem cell migration by the scaffold's internal channels.

Several studies have investigated the effects of supplying growth and regenerative factors with osteochondral repair matrices including those with single-factor transforming growth factor beta 1 (TGF- β 1) releasing capabilities³⁵ and those which can simultaneously release different factors (TGF) and bone morphogenetic protein-2 (BMP-2) from each respective scaffold segment.²³ Sherwood et al.³⁶ were able to show, however, that functionally grading an osteochondral repair structure (poly(L-lactide-co-glycolide)-poly(L-lactide)- β -TCP composite) could be sufficient in guiding chondrocytes to preferentially attach to the cartilage portion of the plug. Another recent study³⁷ has also proven that acellular multilayered polymeric scaffolds alone, with layers graded and tailored to specific tissue types, are just as capable of recruiting host cells for the treatment of osteochondral lesions in a caprine model. The

strategically designed features of the osteochondral plug in this study also reflect this principle.

The highly porous osteochondral plugs used in this study were also able to withstand the biomechanical forces they had been subjected to. This indicated that the previously determined scaffold average Young's modulus value of around 100 kPa was sufficient as all plugs, apart from one exception in an experimental animal, where the plug did not collapse but failed to support tissue growth. A study conducted by Bernstein et al.³⁸ investigated a microporous pure β -TCP ceramic tissue engineering scaffold for the repair of osteochondral defects in a sheep study. Histological, histomorphometric, and immunohistological methods as well as various imaging techniques (X-ray, micro-CT, and scanning electron microscopy) were used to reveal that collagen Type II-positive hyaline cartilage and new subchondral bone had formed in several samples. However, even after 1 year post-implantation, cartilage ingrowth to the center of the defect site was still not completed. Compared to the 8 mm \times 8 mm defects created in the animals of this study, defect sites were 7 mm \times 25 mm in this study. This raises the importance of considering polymeric composites with ceramic materials, where mechanical stability of an acceptable degree is maintained concurrent to the provision of a microarchitecture more accommodating for cells.³⁹

The positive results from the histological analyses also confirmed the biocompatibility of the osteochondral repair material. As such, this *in vivo* study provides a satisfactory preclinical biocompatibility and functionality evaluation of these scaffolds, indicating a strong potential for the clinical uptake of this plug. The "cell-free" material developed and tested in this study may in the future also be reconstituted with a patient's blood or serum for enhanced effects or even serve as an autologous chondrocyte transplantation (ACT)-based cell delivery structure. MaioRegen[®] (Fin-Ceramica Faenza SpA, Faenza, Italy) consists of a collagen Type I top layer that resembles cartilaginous tissue. The bottom layer is composed primarily of magnesium-enriched hydroxyapatite (Mg-HA) that mimics subchondral bone structure.⁴⁰ TruFit[™] Plug (Smith & Nephew, Andover, MA) is also a biphasic plug fabricated from PLGA fibers and calcium sulfate (CaSO₄). The clinical success of MaioRegen has been confirmed by several clinical studies,⁴¹⁻⁴³ but it has also received some contradictory reviews.⁴⁴ The clinical effects of TruFit Plug have been more controversial, with one investigation⁴⁵ finding that compared to traditional treatments or mosaicplasty/microfracture techniques, TruFit Plug did not appear to achieve better results. The OsseoFit[®] plug (Kensey Nash, Exton, PA) is also a biphasic osteochondral repair matrix that is also bioresorbable. Its cartilage-interacting portion is composed of Type I collagen (bovine mesh), while the bone-interacting portion consists of TCP and PLA. A study comparing the TruFit Plug and OsseoFit plug found that the OsseoFit plug was much more malleable and suffered from greater reductions in

height under cyclic loading conditions than the TruFit Plug, but the differences were not statistically significant, potentially due to the relatively small sample size.⁴⁶ Bilge, Buyukdogan, and Doral reported that the animal and human bodies are bioreactors.^{47,48}

Creating large cartilage defects in the sheep is associated with large total defect volume, as these defects produce a large proportion in the subchondral bone. The critical size defects in ovine animal models have been reported to be as 7 mm.⁴⁹ As defects above 7 mm do not have a self-repair capability, we used an 8-mm defect model in our study.⁵⁰ The animal model used in this study is considered suitable for cartilage defect testing. Limitations of this study include the absence of biomechanical evaluation and Phase 3 and Phase 4 trials. Although surface texture and healed cartilage structures are compared with the other anatomical parts in the knee by arthroscopy, endurance and strength comparisons would be an asset as a control for functional status. In future stages, investigations regarding the drug or growth factor delivery capability of this scaffold, along with its various combinations with chondrocytes or stem cells will be possible.

Conclusion

The osteochondral plugs prepared were successful in supporting the regeneration of tissue in osteochondral defects of sheep. The plugs that were supplemented by hyaluronic acid achieved the best coverage of the defect (>65%) at 3 months post-implantation and full coverage of the defect observed at the 6-month mark. No tissue regeneration was seen in defects that were left empty with limping observed in these animals compared to comfortable movement in other groups. There were no degenerative secondary findings on the trochlea and lateral condyles of the experimental animals, whereas mild to severe degeneration observed in the control animals. The defects appear to heal in the form of a narrow crater, attributed to the continuous delivery of bone marrow components via the internal channels of the osteochondral implants. Thus, the unique design of the scaffold proved to have a significant positive impact on the healing of osteochondral lesions. This study demonstrates the potential of the multilayered biomimetic scaffold in repairing osteochondral defects and regenerating cartilage tissue.' instead of 'This study demonstrates the potential of the multilayered biomimetic scaffold in repairing and regenerating cartilage tissue and osteochondral defects.

Supplementary Information

Video material has been provided with this article to supplement the content described within this article. The video content provides the arthroscopic imaging and magnetic resonance imaging (MRI) results, as well as recordings from the operating theater showing the implantation of plug. The supplementary information is intended to provide more detailed analysis of the osteochondral repair *in vivo*.

Declaration of conflicting interests

The author(s) declared no potential conflicts of interest with respect to the research, authorship, and/or publication of this article.

Funding

The author(s) disclosed receipt of the following financial support for the research, authorship, and/or publication of this article: This study was supported by TUBITAK TEYDEB (Project No. 711730) and BMT Calsis Co.

References

1. Mano JF and Reis RL. Osteochondral defects: present situation and tissue engineering approaches. *J Tissue Eng Regen Med* 2007; 1: 261–273.
2. Cram P, Lu X, et al. Total knee arthroplasty volume, utilization, and outcomes among Medicare beneficiaries, 1991–2010. *J Am Med Assn* 2012; 308(12): 1227–1236.
3. Dijkstra LC, de Bont LG, Boering G, et al. Normal cartilage structure, biochemistry, and metabolism: a review of the literature. *J Oral Maxillofac Surg* 1995; 53: 924–929.
4. Jackson DW, Scheer MJ and Simon TM. Cartilage substitutes: overview of basic science and treatment options. *J Am Acad Orthop Surg* 2001; 9: 37–52.
5. Lotz MK and Kraus VB. New developments in osteoarthritis. Posttraumatic osteoarthritis: pathogenesis and pharmacological treatment options. *Arthritis Res Ther* 2010; 12: 211.
6. Buckwalter JA and Lohmander S. Operative treatment of osteoarthrosis. Current practice and future development. *J Bone Joint Surg Am* 1994; 76: 1405–1418.
7. Chen FS, Frenkel SR and Di Cesare PE. Repair of articular cartilage defects: part II. Treatment options. *Am J Orthop* 1999; 28: 88–96.
8. Newman AP. Articular cartilage repair. *Am J Sports Med* 1998; 26: 309–324.
9. Birdsall PD, Hayes JH, Cleary R, et al. Health outcome after total knee replacement in the very elderly. *J Bone Joint Surg Br* 1999; 81: 660–662.
10. Steadman JR, Briggs KK, Rodrigo JJ, et al. Outcomes of microfracture for traumatic chondral defects of the knee: average 11-year follow-up. *Arthroscopy* 2003; 19: 477–484.
11. Bentley G, Biant LC, Carrington RW, et al. A prospective, randomised comparison of autologous chondrocyte implantation versus mosaicplasty for osteochondral defects in the knee. *J Bone Joint Surg Br* 2003; 85: 223–230.
12. Hangody L and Fules P. Autologous osteochondral mosaicplasty for the treatment of full-thickness defects of weight-bearing joints: ten years of experimental and clinical experience. *J Bone Joint Surg Am* 2003; 85(Suppl. 2): 25–32.
13. Curl WW, Krome J, Gordon ES, et al. Cartilage injuries: a review of 31,516 knee arthroscopies. *Arthroscopy* 1997; 13: 456–460.
14. Williams RJ and Gamradt SC. Articular cartilage repair using a resorbable matrix scaffold. *Instr Course Lect* 2008; 57: 563–571.
15. Aydin HM. A three-layered osteochondral plug: structural, mechanical, and in vitro biocompatibility analysis. *Adv Eng Mater* 2011; 13: B511–B517.
16. Aydin HM, Yang Y, Kohler T, et al. Interaction of osteoblasts with macroporous scaffolds made of PLLA/PCL blends modified with collagen and hydroxyapatite. *Advanced Adv Eng Mater* 2009; 11: B83–B88.

17. Pineda S, Pollack A, Stevenson S, et al. A semiquantitative scale for histologic grading of articular cartilage repair. *Acta Anat* 1992; 143: 335–340.
18. Zhang W, Lian Q, Li D, et al. The effect of interface microstructure on interfacial shear strength for osteochondral scaffolds based on biomimetic design and 3D printing. *Mater Sci Eng C: Mater Biol Appl* 2015; 46: 10–15.
19. Deng T, Lv J, Pang J, et al. Construction of tissue-engineered osteochondral composites and repair of large joint defects in rabbit. *J Tissue Eng Regen Med* 2014; 8: 546–556.
20. Gotterbarm T, Richter W, Jung M, et al. An in vivo study of a growth-factor enhanced, cell free, two-layered collagen-tricalcium phosphate in deep osteochondral defects. *Biomaterials* 2006; 27: 3387–3395.
21. Chen J, Chen H, Li P, et al. Simultaneous regeneration of articular cartilage and subchondral bone in vivo using MSCs induced by a spatially controlled gene delivery system in bilayered integrated scaffolds. *Biomaterials* 2011; 32: 4793–4805.
22. Gao J, Dennis JE, Solchaga LA, et al. Repair of osteochondral defect with tissue-engineered two-phase composite material of injectable calcium phosphate and hyaluronan sponge. *Tissue Eng* 2002; 8: 827–837.
23. Reyes R, Delgado A, Sanchez E, et al. Repair of an osteochondral defect by sustained delivery of BMP-2 or TGFβ1 from a bilayered alginate-PLGA scaffold. *J Tissue Eng Regen Med* 2014; 8: 521–533.
24. Oshima Y, Harwood FL, Coutts RD, et al. Variation of mesenchymal cells in poly(lactic acid) scaffold in an osteochondral repair model. *Tissue Eng Part C: Methods* 2009; 15: 595–604.
25. Qi Y, Du Y, Li W, et al. Cartilage repair using mesenchymal stem cell (MSC) sheet and MSCs-loaded bilayer PLGA scaffold in a rabbit model. *Knee Surg Sports Traumatol Arthrosc* 2014; 22: 1424–1433.
26. Shao XX, Huttmacher DW, Ho ST, et al. Evaluation of a hybrid scaffold/cell construct in repair of high-load-bearing osteochondral defects in rabbits. *Biomaterials* 2006; 27: 1071–1080.
27. Galperin A, Oldinski RA, Florczyk SJ, et al. Integrated bilayered scaffold for osteochondral tissue engineering. *Adv Healthc Mat* 2013; 2: 872–883.
28. Shao X, Goh JC, Huttmacher DW, et al. Repair of large articular osteochondral defects using hybrid scaffolds and bone marrow-derived mesenchymal stem cells in a rabbit model. *Tissue Eng* 2006; 12: 1539–1551.
29. Sotoudeh A, Jahanshahi A, Takhtfooladi MA, et al. Study on nano-structured hydroxyapatite/zirconia stabilized yttria on healing of articular cartilage defect in rabbit. *Acta Cir Bras* 2013; 28: 340–345.
30. Niederauer GG, Slivka MA, Leatherbury NC, et al. Evaluation of multiphase implants for repair of focal osteochondral defects in goats. *Biomaterials* 2000; 21: 2561–2574.
31. Frenkel SR, Bradica G, Brekke JH, et al. Regeneration of articular cartilage—evaluation of osteochondral defect repair in the rabbit using multiphase implants. *Osteoarthritis Cartilage* 2005; 13: 798–807.
32. Verdonk P, Dhollander A, Almqvist KF, et al. Treatment of osteochondral lesions in the knee using a cell-free scaffold. *Bone Joint J* 2015; 97B: 318–323.
33. Nukavarapu SP and Dorcemus DL. Osteochondral tissue engineering: current strategies and challenges. *Biotechnol Adv* 2013; 31: 706–721.
34. Chen P, Tao J, Zhu S, et al. Radially oriented collagen scaffold with SDF-1 promotes osteochondral repair by facilitating cell homing. *Biomaterials* 2015; 39: 114–123.
35. Wei Y, Hu H, Wang H, et al. Cartilage regeneration of adipose-derived stem cells in a hybrid scaffold from fibrin-modified PLGA. *Cell Transplant* 2009; 18: 159–170.
36. Sherwood JK, Riley SL, Palazzolo R, et al. A three-dimensional osteochondral composite scaffold for articular cartilage repair. *Biomaterials* 2002; 23: 4739–4751.
37. Levingstone TJ, Ramesh A, Brady RT, et al. Cell-free multi-layered collagen-based scaffolds demonstrate layer specific regeneration of functional osteochondral tissue in caprine joints. *Biomaterials* 2016; 87: 69–81.
38. Bernstein A, Niemeyer P, Salzman G, et al. Microporous calcium phosphate ceramics as tissue engineering scaffolds for the repair of osteochondral defects: histological results. *Acta Biomater* 2013; 9: 7490–7505.
39. Mayr HO, Klehm J, Schwan S, et al. Microporous calcium phosphate ceramics as tissue engineering scaffolds for the repair of osteochondral defects: biomechanical results. *Acta Biomater* 2013; 9: 4845–4855.
40. Irion VH and Flanigan DC. New and emerging techniques in cartilage repair: other scaffold-based cartilage treatment options. *Oper Tech Sport Med* 2013; 21: 125–137.
41. Filardo G, Kon E, Perdisa F, et al. Osteochondral scaffold reconstruction for complex knee lesions: a comparative evaluation. *Knee* 2013; 20: 570–576.
42. Kon E, Filardo G, Venieri G, et al. Tibial plateau lesions. Surface reconstruction with a biomimetic osteochondral scaffold: results at 2 years of follow-up. *Injury* 2014; 45(Suppl. 6): S121–S125.
43. Kon E, Filardo G, Perdisa F, et al. A one-step treatment for chondral and osteochondral knee defects: clinical results of a biomimetic scaffold implantation at 2 years of follow-up. *J Mater Sci Mater Med* 2014; 25: 2437–2444.
44. Christensen BB, Foldager CB, Jensen J, et al. Poor osteochondral repair by a biomimetic collagen scaffold: 1- to 3-year clinical and radiological follow-up. *Knee Surg Sports Traumatol Arthrosc* 2016; 24: 2380–2387.
45. Verhaegen J, Clockaerts S, Van Osch GJ, et al. TruFit plug for repair of osteochondral defects—where is the evidence? Systematic review of literature. *Cartilage* 2015; 6: 12–19.
46. Elguizaoui S, Flanigan DC, Harris JD, et al. Proud osteochondral autograft versus synthetic plugs—contact pressures with cyclical loading in a bovine knee model. *Knee* 2012; 19: 812–817.
47. Buyukdogan K, Doral MN, Bilge O, et al. Peritoneum and omentum are natural reservoirs for chondrocytes of osteochondral autografts: a comparative animal study. *Acta Orthop Traumatol Turc* 2016; 50: 539–543.
48. Bilge O, Doral MN, Atesok K, et al. The effects of the synovium on chondrocyte growth: an experimental study. *Knee Surg Sports Traumatol Arthrosc* 2011; 19: 1214–1223.
49. Ahern BJ, Parvizi J, Boston R, et al. Preclinical animal models in single site cartilage defect testing: a systematic review. *Osteoarthritis Cartilage* 2009; 17: 705–713.
50. US Food and Drug Administration. Cellular products for joint surface repair. In: *Briefing document: cellular, tissue, and gene therapies advisory committee*, 3–4 March 2005, https://www.fda.gov/ohrms/dockets/ac/05/briefing/2005-4093B1_01.pdf